Mg-doping into boron icosahedral cluster solids, targeting high temperature superconductivity

H. Hyodo[1], S. Hosoi[1], S. Araake[1], K. Soga[2], Y. Sato[3], M. Terauchi[3], K. Kimura[1]

[1] Department of Advanced Materials Science, Graduate School of Frontier Sciences, The University of Tokyo,
502/5A5, 5-1-5 Kashiwanoha, Kashiwa, Chiba 277-8561, Japan
+81-4-7316-3759, hyodo@phys.mm.t.u-tokyo.ac.jp
[2] Department of Materials Science and Technology, Tokyo University of Science, Chiba 278-8510, Japan
[3] Institute for Multidisciplinary Research for Advanced Materials, Tohoku University, Sendai 980-8577, Japan

Abstract

High-T_C superconductivity may be possible upon metallic-element doping into boron icosahedral cluster solids. We attempted magnesium (Mg) doping into α-rhombohedral boron (α-B_{12}) and β-rhombohedral boron (β-B_{105}), and discussed the possibility of metal transition and superconductivity. Although the preparation of Mg-doped α-B_{12} cannot be achieved, we achieved Mg doping into β-B_{105} at a high Mg concentration of up to $MgB_{11.5}$ (8.6 Mg/cell), which is the highest metal concentration of β-B_{105} up to now. However, neither metal transition nor superconductivity was observed. We estimated the density of states (DOS) near E_F and discussed the electronic states of β-B_{105}. From the result, it is suggested that a localized state exists above the intrinsic acceptor level probably originating from the B_{28} cluster with structural defects.
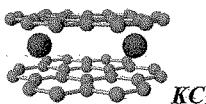
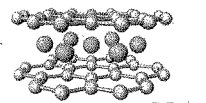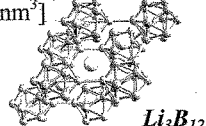Key words: Boron, Cluster solids, Superconductivity, Intercalate

1. INTRODUCTION

Boron (B)-rich solids have a framework crystal structure built up from B_{12} icosahedral clusters. These solids are called boron-icosahedral cluster solids (B-ICSs). B-ICSs have relatively large interstitial doping sites; thus, they can accept a large amount of other elements. The high symmetry of the B_{12} cluster gives rise to the high degeneracy of the electronic states, which accordingly results in the high density of states (DOS). If we can dope metallic elements into B-ICSs and adjust the Fermi energy (E_F) to a position of high DOS, high-T_C superconductivity can be expected[1]. Table I shows a comparison between the layered solids and the cluster solids based on B and carbon (C). In the case of C-rich solids, K_3C_{60} has a much higher T_C[2] than KC_8[3], a layered solid. One of this reason is higher DOS at E_F ($N(E_F)$) of K_3C_{60}[4] than that of KC_8[5] owing to the high symmetry of C_{60} clusters. On the other hand, MgB_2 has a much higher T_C[6] than the similarly layered KC_8. One can

expect higher T_C, due to higher $N(E_F)$, for metal-doped B-ICSs[1] than for layered MgB_2[7] as in the case of C-rich solids. According to first-principles calculations, lithium (Li)-doped α-rhombohedral B (see Table I) is predicted to have higher $N(E_F)$ than K_3C_{60} and MgB_2, and to show superconductivity[1]. Moreover, B-ICSs have not only high $N(E_F)$ values but also high phonon frequencies[8] and a large electron-phonon coupling constant[9] comparable to those of MgB_2. B-ICSs have favorable features for achieving high-T_C superconductivity.

B forms four allotropes: α- and β-rhombohedral B (α-B_{12} and β-B_{105}), and α- and β-tetragonal B, all of which consist of B_{12} clusters. Figure 1 shows the structures of α-B_{12} and β-B_{105} with major doping sites. α-B_{12} has only a B_{12} cluster, on the other hand, β-B_{105} has four B_{12} clusters, single B atom and two B_{28} clusters, which are modified trios consisting of B_{12} clusters in

TABLE I: Superconductivities of layered and cluster solids based on boron and carbon. The $N(E_F)$ values were calculated by referring to Refs. 5, 4, 7 and 1 for KC_8, K_3C_{60}, MgB_2 and Li_3B_{12}, respectively.

	Layered Solids		Cluster Solids	
Carbon	KC_8: $T_c \sim 0.1$ [K] $N(E_F) \sim 14$ [states/eV nm^3] $\omega \sim 170$ [cm^{-1}]	KC_8	K_3C_{60}: $T_c \sim 20$ [K] $N(E_F) \sim 25$ [states/eV nm^3] $\omega \sim 500 - 1400$ [cm^{-1}]	K_3C_{60}
Boron	MgB_2: $T_c \sim 40$ [K] $N(E_F) \sim 24$ [states/eV nm^3] $\omega \sim 600$ [cm^{-1}]	MgB_2	Li_3B_{12}: $N(E_F) \sim 39$ [states/eV nm^3] $\omega \sim 500 - 1200$ [cm^{-1}] $Mg_xB_{12}, Mg_xB_{105}, Mg_xB_{50}$, $T_c > 40$ K?	Li_3B_{12}

rhombohedral unit cell. The ideal structural formula of β-B_{105} is given as $(B_{12})_4(B_{28})_2B$, however, it has partially occupied sites, i.e., the occupancy of B(B13) is approximately 75% and those of B(B16) to B(B20) are 3-25%. Therefore, the actual structural formula of β-B_{105} becomes $B_{106.6}$[10]; however, we call β-rhombohedral boron β-B_{105} for convenience. α-B_{12} cannot be easily prepared experimentally. α-B_{12} can only be prepared at temperatures below approximately 1470 K, which is approximately 1000 K lower than the melting point of B. Above this temperature, an irreversible transformation from α-B_{12} to β-B_{105} takes place.

Li or Mg was not doped wholly, but doped only in small part of the samples into α-B_{12} by vapor diffusion processing (VDP). The possibility of superconductivity was observed at 36 K[11]. On the other hand, Li[12] or Mg[11] were doped into β-B_{105} by VDP, however, the samples remained semiconductor. Li doping into β-B_{105}, only causes the filling of the intrinsic acceptor level (IAL)[13] which is a gap state and can accept at most 8 electrons/cell[12]. The origin of the IAL is considered to be the electron-deficiency of B_{12}, the Jahn-Teller effect[14,15] and structural defects[16,17]. Thus, if we can dope more than 8 electrons per unit cell into β-B_{105}, metal transition and superconductivity can be expected.

We attempted Mg doping aiming at metal transition and superconductivity by large amount of electron doping. In this study, we report Mg doping into α-B_{12} and β-B_{105}, and discuss the possibility of metal transition and superconductivity of Mg doped B-ICSs.

2. EXPERIMENT

α-B_{12} is prepared using crystallization by annealing of amorphous boron (am-B). Thus, we tried to synthesize Mg-doped α-B_{12} by annealing of am-B under Mg vapor. Because Mg reacts with quartz tube by annealing near 1470K[11], the crystallization temperature of α-B_{12}, we used stainless tube instead of quartz tube. Am-B powder (4 N purity) were put in a hexagonal boron nitride (BN) crucible. The crucible and Mg granules (3 N purity) were put in a stainless tube, and then the tube was sealed by arc welding under argon atmosphere. The tube was heated at 1453-1573 K for 1-100 h.

β-B_{105} powder (2 N or 5 N purity) and Mg granules (3 N purity) were placed at both ends of a BN crucible, and a BN spacer was placed to separate B and Mg. The crucible was sealed in an evacuated quartz tube and heated at 973-1473 K for 1-100 h. To measure the electrical conductivity, some samples were sintered by spark plasma sintering (SPS) at 1273 K for 10 min.

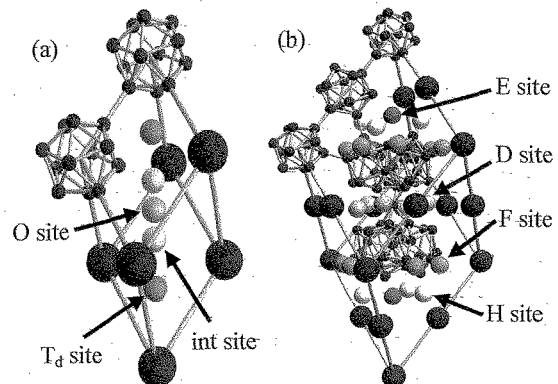The samples were investigated by XRD with CuKα radiation and analyzed by the Rietveld method using the

FIG. 1: Structures of (a) α-B_{12} and (b) β-B_{105} with major doping sites. α-B_{12} has only a B_{12} cluster; on the other hand, β-B_{105} has not only B_{12} clusters but also B_{28} clusters as building blocks.

program RIETAN-2000[18]. The magnetic susceptibility was measured using a SQUID magnetometer at 1 T from 2 to 300 K, and under conditions of zero-field cooling (ZFC) and field cooling (FC) at 10 Oe from 2 to 100 K to examine superconductivity. The electrical conductivity was measured from 50 to 300 K using the van der Pauw method.

3. RESULTS AND DISCUSSION

3.1 α-rhombohedral boron

Mg-doped α-B_{12} was not obtained by annealing of am-B under Mg vapor. Only MgO, MgB_2 and MgB_4 were synthesized and even Mg-doped β-B_{105} was not crystallized. The crystallization of α-B_{12} is influenced a great deal by impurities and annealing temperature[19]. The crystallization of Mg-doped α-B_{12} may be the same case and our condition of them may not be suitable.

3.2 β-rhombohedral boron

For the Rietveld refinement, we assumed the doping sites for Mg to be the D, E, F and the recently suggested the H site[20]. Table II shows the VDP or SPS conditions, the composition of the unit cell, the occupancies of the partially occupied sites, and the reliability factor R_{wp} of selected samples. Mg was successfully doped at a high concentration into β-B_{105} without Si doping, up to $MgB_{11.5}$ (8.6 Mg/cell), by annealing at less than 1273 K. It is considered that we achieved electron doping over the IAL of up to approximately 17 electrons/cell. We measured Mg-β-B 2 using synchrotron radiation powder diffraction (SR)[21]. The result of Rietveld refinement (see Table II) is almost consistent with the result of conventional XRD. The sintered samples prepared for

TABLE II: VDP or SPS conditions, compositions of unit cell, occupancies of partially occupied sites and reliability factor R_{wp}. Mg-β-B 2 (SPS) was prepared by SPS from Mg-β-B 2. The result of our SR[21] data is also shown.

Sample namte	VDP/SPS condition	Composition	Occupancy [%]						R_{wp}
			Mg(D)	Mg(E)	Mg(F)	Mg(H)	B(B4)	B(B13)	
Mg-β-B 1	1273K 10h	$Mg_{4.7}B_{101}$	43.5(6)	91(1)	5(7)	0	92(2)	56(2)	12.2
Mg-β-B 2	1073K 10h	$Mg_{7.9}B_{99}$	62.0(5)	86.0(8)	23.8(7)	17.2(5)	71(2)	61(2)	12.5
Mg-β-B 2 (SR)	1073K 10h	$Mg_{7.8}B_{101}$	60.2	86.1	21.6	19.7	83.0	69.8	2.9
Mg-β-B 3	1073K 10h	$Mg_{8.6}B_{99}$	63.1(6)	80.3(9)	28.0(9)	25.6(4)	67(2)	68(2)	7.8
Mg-β-B 2 (SPS)	1273K 10min	$Mg_{7.7}B_{100}$	63.9(4)	88.4(6)	24.2(7)	7.7(4)	71(1)	65(2)	9.7

electrical conductivity measurements were crushed and analyzed by XRD. No defection of Mg due to sintering occurred (see Table II). Figures 2(a) and (b) show the relationships between the occupancies of Mg(F) and B(B4) and Mg(H) and Mg(E), respectively. It is confirmed that Mg(F) is doped with substituting B(B4). The occupancy of Mg(E) decreased with Mg doping in large amounts. This is because Mg moved from the E site to the H site whose multiplicity is three times higher than that of the E site to accept more Mg.

Although we measured the magnetic susceptibility of Mg-doped β-B_{105} from 2 to 100 K under conditions of ZFC and FC, no indication of superconductivity was observed. Figure 3 shows the temperature dependence of the magnetic susceptibility χ of undoped and Mg-doped β-B_{105}. χ was analyzed using

$$\chi = \chi_0 + \chi_{CW} + \chi_F(T) = \chi_0 + \frac{C}{T - \theta_p} + \frac{AT + B}{H}, \quad (1)$$

where χ_0 is a temperature-independent term. The second term χ_{CW} is a term that obeys the Curie-Weiss law. The third term $\chi_F(T)$ is a ferromagnetism term represented by saturation magnetization M_S over H, because the measurements were performed under a magnetic field that was stronger than the saturation magnetic field. χ_{CW} and $\chi_F(T)$ originate from impurities. Because the M_S has a linear temperature dependence in this temperature range, we assumed that $M_S = AT + B = \chi_F(T) \times H$, where A and B are proportionality constants. The data in Fig. 3 were fitted using Eq. (1), and χ_0 was obtained as a fitting parameter.

$\Delta\chi_0$, the change in χ_0 due to the doping, is given as

$$\Delta\chi_0 = \Delta\chi_p + \Delta\chi_L = \mu_B^2 \Delta N(E_F) \left\{ 1 - \frac{1}{3}\left(\frac{m}{m^*}\right)^2 \right\}, \quad (2)$$

where χ_p is the Pauli paramagnetism, χ_L is the Landau diamagnetism, $\Delta N(E_F)$ is the difference in $N(E_F)$ caused by the doping and m^* is the effective mass; we assumed that $m^* = m$. The relationship between the number of doped electrons and $\Delta N(E_F)$ was investigated[22]. Our previous results of Li doping and the codoping of Mg and Si into β-B_{105} was also considered[11,12]. To determine the number of doped electrons per atom, it was assumed that Li and Mg donate 1 and 2 electrons, respectively, and Si replacing a B atom donates 1 electron. This dependence of $\Delta N(E_F)$ on the number of doped electrons is discussed later with the results of the electrical conductivity.

Figure 4 shows the temperature dependence of the electrical conductivity σ of undoped and Mg-doped β-B_{105}. σ increased by several orders of magnitude with Mg doping, but it still showed variable-range hopping (VRH) behavior as in the case of β-B_{105} and Li-doped β-B_{105}. Therefore, the E_F was in the localized state and even the metal transition was not observed for the sample doped with more than 4 Mg/cell, for which it is considered that E_F reaches the conduction band over the IAL. According to Mott's law for three-dimensional VRH conduction, σ is given as
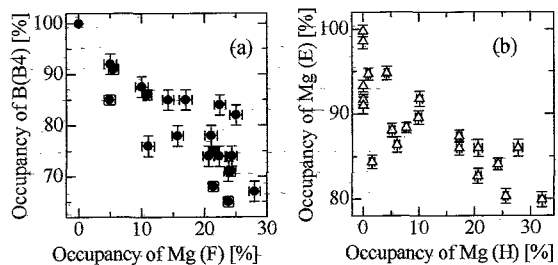

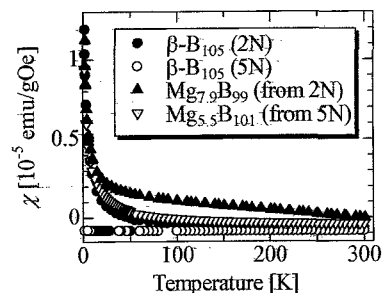FIG. 2: Relationships between occupancies of (a) Mg(F) and B(B4) and (b) Mg(H) and Mg(E).

FIG. 3: Temperature dependence of magnetic susceptibility χ of undoped and Mg-doped β-B_{105} prepared from 2 N and 5 N materials.
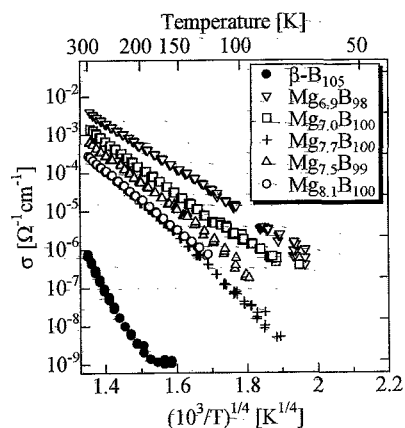

FIG. 4: Temperature dependence of electrical conductivity σ of undoped and Mg-doped β-B_{105}.

$$\sigma = \sigma_0 \exp\left\{ -\left(\frac{T_0}{T}\right)^{\frac{1}{4}} \right\}; \quad \left(T_0 = \frac{60\alpha^3}{\pi k_B N(E_F)} \right), \quad (3)$$

where σ_0 is a constant and α^{-1} is the localization length of the wave function of the carrier. The relationship between the number of doped electrons and $N(E_F)$, which was obtained from the slope of the curve in Fig. 4 was investigated[22]. We also examined our previous results of Li doping and the codoping of Mg and Si into β-B_{105}[11,12].

$\Delta N(E_F)$ can be approximated to be $N(E_F)$, because undoped β-B_{105} is a semiconductor. $N(E_F)$ and $\Delta N(E_F)$

showed almost the same behaviors[22]. The difference between the absolute values of $N(E_F)$ and $\Delta N(E_F)$ may originate from the hypothesis on localization length and effective mass. In the region where the number of doped electrons was less than 8, with increasing number of doped electrons, $N(E_F)$ increased and reached its maximum when the number of doped electrons is approximately 5 (half-filled). With supplying more electrons, $N(E_F)$ turned to decrease and became almost the same value as β-B_{105} when the number of doped electrons is approximately 8 (completely filled). This increasing and decreasing behavior of $N(E_F)$ indicates the filling of the IAL[11].

On the other hand, the increasing and decreasing behavior of $N(E_F)$ in the region where the number of doped electrons is more than 8 indicates the DOS figure at an energy higher than that of the IAL, which is clarified due to Mg doping. With increasing number of doped electrons, $N(E_F)$ showed the increasing and decreasing behavior once more. Therefore, the existence of another localized state above the IAL was indicated. It is because E_F was in this localized state that neither metal transition nor superconductivity was observed, in spite of the electron doping over the IAL.

β-B_{105} also has six electron trapping levels[14-16] as intrinsic gap states. However, the contribution of them to electrical conduction should not be dominant in this system because its hypothesis cannot interpret the experimental results. It is possible that this newfound localized state is the gap state originating from the defection of B(B4) caused by Mg doping, which belongs to the B_{28} cluster. Mg starts to occupy the F site when the number of doped electrons is approximately 8, i.e., B(B4) starts to defect after the IAL has been occupied. It seems that the localized state arises in order for Fermi energy not to reach the conduction band and to keep the energy of the system lower. The complete occupation of this newfound localized state in spite of the parallel increase of the capacity of it and the number of doped electrons from Mg(F), which are proportional to the amount of the defection of B(B4) in this hypothesis, may originate from the occupation of Mg(H), which can donate three times electrons than Mg(E) and accelerate the occupation of this newfound localized state. Mg starts to occupy the H site when the number of doped electrons was approximately 12 where $N(E_F)$ turned to decrease.

However, this possibility is too difficult to discuss in detail at present and now in progress, because it has been shown that Mg doping influences the structural defects that originally exist in β-B_{105}[20,21], which are the origin of the IAL according to Refs. 16 and 17. It was found that it is difficult for β-B_{105} to achieve metal transition and superconductivity because of the localized states originating from the electron deficiency and structural defects in the B_{28} cluster[22].

4. CONCLUSION

Although the crystallization of Mg-doped α-B_{12} can't be achieved, we achieved large amount of Mg doping into β-B_{105}, up to $MgB_{11.5}$ (8.6 Mg/cell). The electron doping over the IAL was achieved. Nevertheless, E_F was in the localized state. This newfound localized state probably originates from the defection of B(B4) which

belongs to the B_{28} cluster. It is difficult for β-B_{105} to achieve metal transition and superconductivity because of the localized states originating from the structural defects in the B_{28} cluster, which is unique to β-B_{105}. We should aim at high-T_C superconductivity using not β-B_{105}, but other B-ICS without B_{28} cluster that includes structural defects, such as α-B_{12} or α-tetragonal $B^{23,24}$.

5. ACKNOWLEDGMENTS

References
[1] S. Gunji and H. Kamimura, Phys. Rev. B **54**, 13665 (1996).
[2] A. F. Hebard, et al., Nature **350**, 600 (1991).
[3] Y. Koike, et al., J. Phys. Chem. **41**, 1111 (1980).
[4] O. Gunnarsson, Rev. Mod. Phys. **69**, 575 (1997).
[5] S. Mizuno, et al., J. Phys. Soc. Jpn. **56**, 4466 (1987).
[6] J. Nagamatu, et al., Nature **410**, 63 (2001).
[7] J. Kortus, et al., Phys. Rev. Lett. **86**, 4656 (2001).
[8] N. Vast, et al., Phys. Rev. Lett. **78**, 693 (1997).
[9] M. Calandra, et al., Phys. Rev. B **69**, 224505 (2004).
[10] G. A. Slack, et al., J. Solid State Chem. **76**, 52 (1988).
[11] H. Matsuda, et al., Phys. Rev. B **52**, 6102 (1995).
[12] K. Soga, et al., J. Solid State Chem. **177**, 498 (2004).
[13] R. Schmechel and H. Werheit, J. Solid State Chem. **154**, 68 (2000).
[14] R. Frantz and H. Werheit, Europhys. Lett. **9**, 145 (1989).
[15] M. Fujimori and K. Kimura, J. Solid State Chem. **133**, 178 (1997).
[16] R Schmechel and H Werheit, J. Phys.: Condens. Matter **11**, 6803 (1999).
[17] Y. Imai, et al., J. Alloys Compd. **347**, 244 (2002).
[18] F. Izumi and T. Ikeda, Mater. Sci. Forum **321**, 198 (2000).
[19] S. O. Shalamberidze, et al., J. Solid State Chem. **154**, 199 (2000).
[20] V. Adasch, et al., J. Solid State Chem. **179**, 2900 (2006).
[21] S. Hosoi, et al., J. Phys. Soc. Jpn. (submitted).
[22] H. Hyodo, et al., Phys. Rev. B (in press).
[23] Z. Wang, et al., Chem. Phys. Lett. **368**, 663 (2003).
[24] K. Kirihara, et al., J. Solid State Chem. **179**, 2799 (2006).